Hydrodynamic force on a particle oscillating in a viscous fluid near a wall with dynamic partial-slip boundary condition

B. U. Felderhof*
Institut für Theoretische Physik A, RWTH Aachen University, Templergraben 55, 52056 Aachen, Germany
(Received 10 February 2012; published 3 April 2012)

The hydrodynamic force on a particle oscillating in a viscous fluid near a wall with partial-slip boundary condition is studied on the basis of the linearized Navier-Stokes equations. Both incompressible and compressible fluids are considered. It is assumed that the slip length characterizing the partial-slip boundary condition depends on frequency. The consequences of this assumption for the spectrum of Brownian motion near a wall are investigated and compared with a recent experiment.

DOI: 10.1103/PhysRevE.85.046303 PACS number(s): 47.15.G−, 47.55.N−, 47.61.−k, 05.40.Jc

I. INTRODUCTION

The boundary condition for the flow velocity of a viscous fluid near a wall has long been a subject of debate in hydrodynamics. In situations on a macroscopic length scale the usual no-slip condition can be used [1]. On the microscale a partial-slip boundary condition for the flow velocity components parallel to the wall must be used, characterized by a slip length of the order of nanometers, or even micrometers [2]. The boundary condition strongly affects the flow of confined fluids [3,4]. Various experimental methods can be used to measure the slip length, including the Poiseuille flow rate, the Poiseuille flow pattern, and fluorescence recovery [5]. The hydrodynamic boundary condition has also been studied in computer simulations from the behavior of time-correlation functions [6–8]. The subject has been reviewed by Lauga *et al.* [2], by Neto *et al.* [9], by Bocquet and Barrat [10], and in the context of nanofluidics [11] by Bocquet and Charlaix [12].

In recent experiments the spectral density of the position fluctuations of Brownian motion of a particle trapped in a harmonic potential well near a wall has been studied [13–16]. The experimental data of Ref. [16] were explained on the basis of an unconvincing approximate expression for the frequency-dependent susceptibility of a particle near a wall with no-slip boundary condition [17]. The correct expression was derived earlier [18], and does not show the initial decrease of the spectrum at low frequency seen experimentally [16], but rather leads to an increase with frequency. We have suggested [19] that a partial-slip boundary condition with frequency-dependent slip length may be responsible for the decrease. In the present article we investigate the consequences of a dynamic partial-slip boundary condition on the spectral density of Brownian motion in more detail.

The earlier calculation of the susceptibility of a particle near a wall with no-slip condition, for both an incompressible [18] and a compressible fluid [20], is extended to the case of a wall with partial-slip boundary condition. As a bonus we find the steady-state mobility of the particle as a function of the slip length at zero frequency [21,22], in generalization of the result derived by Lorentz [23] for the no-slip condition. The steady-state mobility is independent of fluid compressibility.

The calculation is valid to first order in the ratio of particle radius and distance to the wall. The approximation may be expected to be accurate provided the ratio is larger than about 5. Corrections due to finite particle size can be evaluated in principle, but require elaborate calculation [24]. The problem involves the calculation of the Green function of the linearized Navier-Stokes equations in the presence of a wall with the boundary condition, and is similar to the problem in electrodynamics of a dipole radiating above the earth, solved by Sommerfeld [25,26] in the early days of radio. We use a different method based on work by Jones [27] for the steady-state Stokes equations. The solution can be extended to the case with two planar walls [28].

It has been shown experimentally that the slip length characterizing the partial-slip boundary condition depends strongly on the rate of shear [29,30]. It has been suggested by Zwanzig [31] that there is a connection between the non-Newtonian dependence of viscosity on the shear rate and the frequency dependence of the Newtonian viscosity. In analogy, we consider a slip length which depends on frequency. It turns out that the spectral density of Brownian motion depends strongly on the parameters characterizing the frequency dependence of the slip length. This suggests that the analysis of Brownian motion, especially for motions parallel to the wall, can be a useful tool for the investigation of the partial-slip boundary condition. Atomic force microscopy with use of a microsphere provides an interesting alternative [32,33].

II. LINEAR HYDRODYNAMICS

We consider a spherical particle of radius a and mass m_p, immersed in a viscous incompressible fluid of shear viscosity η and mass density ρ. The fluid is bounded by a planar wall and confined to the half space $z > 0$. The fluid is assumed to satisfy a partial-slip boundary condition at the wall and a no-slip boundary condition at the surface of the sphere. The particle is confined to a harmonic trap with force constant k, and subjected to a time-dependent force $\boldsymbol{E}(t)$ acting at the center $\boldsymbol{R}(t)$ of the particle. The force will be assumed to be small, so that we can use linearized equations of motion. The center of the particle performs small motions about the rest position $\boldsymbol{r}_0$.

For small-amplitude motion the flow velocity $\boldsymbol{v}(\boldsymbol{r},t)$ and the pressure $p(\boldsymbol{r},t)$ are governed by the linearized Navier-Stokes

*ufelder@physik.rwth-aachen.de

equations

$$\rho\frac{\partial \boldsymbol{v}}{\partial t}=\eta\nabla^2\boldsymbol{v}-\nabla p,\quad \nabla\cdot\boldsymbol{v}=0. \tag{2.1}$$

The pressure $p(\boldsymbol{r},t)$ is determined by the condition of incompressibility. After Fourier analysis in time we find that the equations for the Fourier components with time factor $\exp(-i\omega t)$ are

$$\eta(\nabla^2\boldsymbol{v}_\omega-\alpha^2\boldsymbol{v}_\omega)-\nabla p_\omega=0,\quad \nabla\cdot\boldsymbol{v}_\omega=0, \tag{2.2}$$

where we have used the abbreviation

$$\alpha=(-i\omega\rho/\eta)^{1/2},\quad \mathrm{Re}(\alpha)>0. \tag{2.3}$$

The equation of motion for the particle may be written in Fourier language as

$$-i\omega(m_p-m_f)\boldsymbol{U}_\omega=-\boldsymbol{\mathcal{F}}_\omega-k\boldsymbol{R}_\omega+\boldsymbol{E}_\omega, \tag{2.4}$$

where $m_f=4\pi a^3\rho/3$ is the mass of fluid displaced by the sphere, and $\boldsymbol{\mathcal{F}}_\omega$ is the total induced force exerted by the particle on the fluid [34].

In the point-particle limit the induced force becomes

$$\boldsymbol{\mathcal{F}}_\omega=\left[6\pi\eta a(1+\alpha a)-\tfrac{3}{2}i\omega m_f\right][\boldsymbol{U}_\omega-\mathsf{F}(\boldsymbol{r}_0,\omega)\cdot\boldsymbol{E}_\omega], \tag{2.5}$$

where $\mathsf{F}(\boldsymbol{r}_0,\omega)$ is the reaction field tensor, defined by [18]

$$\mathsf{F}(\boldsymbol{r}_0,\omega)=\lim_{\boldsymbol{r}\to\boldsymbol{r}_0}[\mathsf{G}(\boldsymbol{r},\boldsymbol{r}_0,\omega)-\mathsf{G}_0(\boldsymbol{r}-\boldsymbol{r}_0,\omega)], \tag{2.6}$$

where $\mathsf{G}(\boldsymbol{r},\boldsymbol{r}_0,\omega)$ is the Green function for the geometry under consideration, and $\mathsf{G}_0(\boldsymbol{r}-\boldsymbol{r}_0,\omega)$ is the Green function for infinite space. Substituting this into the equation of motion (2.4) and solving for the velocity $\boldsymbol{U}_\omega$, we obtain

$$\boldsymbol{U}_\omega=\boldsymbol{\mathcal{Y}}(k,\boldsymbol{r}_0,\omega)\cdot\boldsymbol{E}_\omega, \tag{2.7}$$

where the admittance tensor $\boldsymbol{\mathcal{Y}}(k,\boldsymbol{r}_0,\omega)$ in the presence of the trap is related to that in the absence of the trap by [14]

$$\boldsymbol{\mathcal{Y}}(k,\boldsymbol{r}_0,\omega)=\left[\boldsymbol{\mathcal{Y}}(0,\boldsymbol{r}_0,\omega)^{-1}-\frac{k}{i\omega}\mathsf{I}\right]^{-1}, \tag{2.8}$$

with unit tensor I. The admittance tensor in the absence of the trap is given by [18]

$$\boldsymbol{\mathcal{Y}}(0,\boldsymbol{r}_0,\omega)=\mathcal{Y}_0(\omega)\left[\mathsf{I}+6\pi\eta a\left(1+\alpha a+\tfrac{1}{3}\alpha^2a^2\right)\mathsf{F}(\boldsymbol{r}_0,\omega)\right], \tag{2.9}$$

where $\mathcal{Y}_0(\omega)$ is the scalar admittance for infinite space [35],

$$\begin{aligned}\mathcal{Y}_0(\omega)&=\left[-i\omega m_p+6\pi\eta a\left(1+\alpha a+\tfrac{1}{9}\alpha^2a^2\right)\right]^{-1}\\&=\left[-i\omega\left(m_p+\tfrac{1}{2}m_f\right)+\zeta(\omega)\right]^{-1},\\ \zeta(\omega)&=6\pi\eta a(1+\alpha a).\end{aligned} \tag{2.10}$$

Here the term $\frac{1}{2}m_f$ is the added mass.

III. REACTION FIELD TENSOR

The Green function for infinite space is translationally invariant and given explicitly by [24]

$$\mathsf{G}_0(\boldsymbol{r},\omega)=\frac{1}{4\pi\eta}\left(\frac{e^{-\alpha r}}{r}\mathsf{I}+\alpha^{-2}\nabla\nabla\frac{1-e^{-\alpha r}}{r}\right). \tag{3.1}$$

In order to calculate the Green function $\mathsf{G}(\boldsymbol{r},\boldsymbol{r}_0,\omega)$ in the presence of a wall at $z=0$ with partial-slip boundary condition characterized by slip length b,

$$(\mathsf{I}-\boldsymbol{e}_z\boldsymbol{e}_z)\cdot\boldsymbol{v}|_{z=0}=b\,\boldsymbol{e}_z\cdot(\nabla\boldsymbol{v}+\widetilde{\nabla\boldsymbol{v}})\cdot(\mathsf{I}-\boldsymbol{e}_z\boldsymbol{e}_z)|_{z=0}, \tag{3.2}$$

and with kinematic condition

$$\boldsymbol{e}_z\cdot\boldsymbol{v}|_{z=0}=0, \tag{3.3}$$

we employ the method developed by Jones [27] for the case $\omega=0$. The term with $\widetilde{\nabla\boldsymbol{v}}$ in Eq. (3.2) does not contribute because of Eq. (3.3).

By translational symmetry we expect $\mathsf{G}(\boldsymbol{r},\boldsymbol{r}_0,\omega)$ to depend only on the differences $x-x_0$ and $y-y_0$, so that we can introduce a two-dimensional Fourier transform in the xy plane. With two-dimensional position vectors $\boldsymbol{s}=(x,y)$ and $\boldsymbol{s}_0=(x_0,y_0)$, we express $\mathsf{G}(\boldsymbol{r},\boldsymbol{r}_0,\omega)$ as $\mathsf{G}(\boldsymbol{s}-\boldsymbol{s}_0,z,z_0,\omega)$ and transform it as

$$\mathsf{G}(\boldsymbol{s}-\boldsymbol{s}_0,z,z_0,\omega)=\int d\boldsymbol{q}\;e^{i\boldsymbol{q}\cdot(\boldsymbol{s}-\boldsymbol{s}_0)}\hat{\mathsf{G}}(\boldsymbol{q},z,z_0,\omega). \tag{3.4}$$

The undisturbed particle position is taken as $\boldsymbol{r}_0=(0,0,h)$. The elements $G_{\alpha\beta}(\boldsymbol{r},\boldsymbol{r}_0,\omega)$ of the Green tensor can be found from the solution of ordinary differential equations, in the same way as for the no-slip boundary condition [18]. For our purpose it suffices to consider the elements $\hat{G}_{xx}(\boldsymbol{q},z,h,\omega)$ and $\hat{G}_{zz}(\boldsymbol{q},z,h,\omega)$.

We write the relevant elements of the reaction field tensor, defined in Eq. (2.6), in the form

$$F_{xx}(h,\omega)=\frac{1}{4\pi\eta h}X,\quad F_{zz}(h,\omega)=\frac{1}{4\pi\eta h}Z, \tag{3.5}$$

with dimensionless functions X and Z. These functions are found as integrals over wave number q arising from the Fourier transforms in the x and y directions,

$$X=h\int_0^\infty f_x(q,\omega)q\,dq,\quad Z=h\int_0^\infty f_z(q,\omega)q\,dq. \tag{3.6}$$

The integrands can be written as fractions,

$$f_x(q,\omega)=\frac{N_x(q,\omega)}{D_x(q,\omega)},\quad f_z(q,\omega)=\frac{N_z(q,\omega)}{D_z(q,\omega)}. \tag{3.7}$$

We introduce the abbreviations

$$n=\exp[qh],\quad u=\exp[sh],\quad s=\sqrt{q^2+\alpha^2}. \tag{3.8}$$

The numerator $N_x(q,\omega)$ takes the form

$$\begin{aligned}N_x(q,\omega)&=4nuqs^2(1+sb)-u^2qs(q+s)[1+(s-q)b]\\&\quad\times(1+sb)+n^2[q^2s(1-3s^2b^2)-2qs^3b\\&\quad-q^3(1+qb)(1-sb)-2s^3(1-s^2b^2)].\end{aligned} \tag{3.9}$$

The denominator $D_x(q,\omega)$ takes the form

$$D_x(q,\omega)=2\alpha^2n^2u^2s(s-q)(1+sb)[1+(q+s)b]. \tag{3.10}$$

The numerator $N_z(q,\omega)$ takes the form

$$\begin{aligned}N_z(q,\omega)&=4nuq^2s-u^2qs(q+s)[1+(s-q)b]\\&\quad-n^2q^2(q+s)[1+(q-s)b].\end{aligned} \tag{3.11}$$

The denominator $D_z(q,\omega)$ takes the form

$$D_z(q,\omega)=\alpha^2n^2u^2s(s-q)[1+(q+s)b]. \tag{3.12}$$

It is convenient to express the functions X and Z as

$$X = X(v,w), \quad Z = Z(v,w), \tag{3.13}$$

with dimensionless variables

$$v = \alpha h, \quad w = b/h. \tag{3.14}$$

In the no-slip limit $b = 0$ the expressions simplify. In this limit the integrals over wave number q in Eq. (3.6) can be performed [18], so that $X_0 = X(v,0)$ and $Z_0 = Z(v,0)$ are known in explicit form.

In the perfect-slip limit $b \to \infty$, the integrands in Eq. (3.6) become

$$f_{xs}(q,\omega) = \frac{n^2(2s^2 - q^2) - qsu^2}{2\alpha^2 n^2 u^2 s}, \qquad f_{zs}(q,\omega) = \frac{q(n^2 q - u^2 s)}{\alpha^2 n^2 u^2 s}. \tag{3.15}$$

The integrals in Eq. (3.6) can be performed, and take the values

$$X_s = X(v,\infty) = \frac{-1}{8v^2}[1 - (1 + 2v + 4v^2)e^{-2v}], \qquad Z_s = Z(v,\infty) = \frac{-1}{4v^2}[1 - (1 + 2v)e^{-2v}], \tag{3.16}$$

in agreement with the result obtained by the method of images [36].

IV. STEADY-STATE MOBILITY AND LOW-FREQUENCY BEHAVIOR

In the steady-state limit $\omega \to 0$ the expressions simplify. The integrand $f_x(q,\omega)$ becomes

$$f_x(q,0) = -\frac{3 + qb - 6q^2b^2 - qh(1 - qb - 2q^2b^2) + 2q^2h^2(1 + qb)}{4q(1 + qb)(1 + 2qb)}\, e^{-2qh}, \tag{4.1}$$

with the corresponding integral in Eq. (3.6)

$$X(0,w) = \frac{1}{16w^2}(1 + 3w + 4w^2) - \frac{1}{16w^3}(1 + 2w)^2 \times e^{1/w}\, E_1(1/w) - \frac{1}{w}e^{2/w}\, E_1(2/w). \tag{4.2}$$

The integrand $f_z(q,\omega)$ becomes

$$f_z(q,0) = -\frac{1 + 2qb + qh(1 + 2qb) + 2q^2h^2}{2q(1 + 2qb)}\, e^{-2qh}, \tag{4.3}$$

with the corresponding integral in Eq. (3.6)

$$Z(0,w) = \frac{1}{8w^2}(1 - w - 4w^2) - \frac{1}{8w^3}e^{1/w}\, E_1(1/w). \tag{4.4}$$

The steady-state mobility for transverse and perpendicular motion is given by [21,22]

$$\mu_{xx} = \mu_0\left[1 + \frac{3a}{2h}X(0,w)\right], \quad \mu_{zz} = \mu_0\left[1 + \frac{3a}{2h}Z(0,w)\right], \tag{4.5}$$

where $\mu_0 = 1/(6\pi\eta a)$.

In the limit $b \to 0$, corresponding to the no-slip boundary condition, the above expressions become

$$X(0,0) = -\tfrac{3}{8}, \quad Z(0,0) = -\tfrac{3}{4}, \tag{4.6}$$

in agreement with the values derived by Lorentz for the zero-frequency mobility [23]. In the limit $b \to \infty$, corresponding to the perfect-slip boundary condition, the expressions become

$$X(0,\infty) = \tfrac{1}{4}, \quad Z(0,\infty) = -\tfrac{1}{2}, \tag{4.7}$$

in agreement with the values derived from Eq. (3.16). In Fig. 1 we plot the functions $X(0,w)$ and $Z(0,w)$ as functions of w. The function $X(0,w)$ changes sign at $w_0 = 5.4524$.

The low-frequency behavior of the reaction field factors $F_{xx}(h,\omega)$ and $F_{zz}(h,\omega)$ can be obtained from the expansion of the functions $X(v,w)$ and $Z(v,w)$ in powers of v. In the limits $w \to 0$ and $w \to \infty$, these can be obtained from the explicit values of the integrals. For intermediate values of w the term linear in v can be obtained from an asymptotic analysis of the integrals. The low-frequency behavior is determined by the behavior of the functions $f_x(q,\omega)$ and $f_z(q,\omega)$ for small q and ω. We use the method developed in Ref. [28]. Substituting $q = q'\varepsilon$ and $\omega = i\varepsilon^2$ and expanding the numerator N_x and denominator D_x in powers of ε, we obtain

$$f_x(q,\omega) \approx -\frac{1}{\alpha^2}\sqrt{q^2 + \alpha^2} + \frac{q^2}{2\alpha^2\sqrt{q^2 + \alpha^2}} + \frac{q}{2\alpha^2}, \tag{4.8}$$

independent of the slip length b. Similarly we obtain

$$f_z(q,\omega) \approx \frac{q^2}{\alpha^2\sqrt{q^2 + \alpha^2}} - \frac{q}{\alpha^2}, \tag{4.9}$$

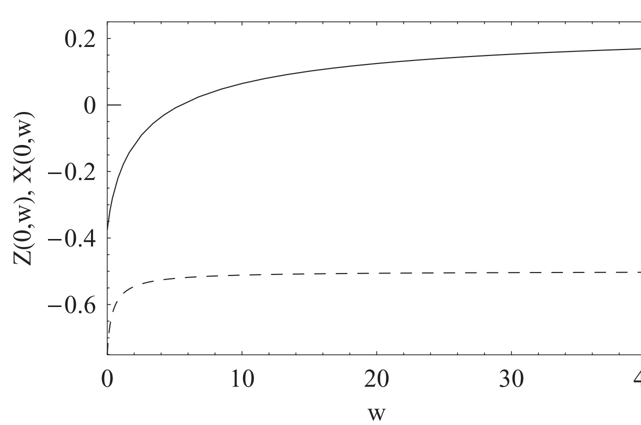

FIG. 1. Dimensionless functions $X(0,w)$ (solid curve) and $Z(0,w)$ (dashed curve) as functions of the parameter $w = b/h$, where b is the slip length, and h is the distance to the wall. The particle mobility is given by Eq. (4.5).

again independent of b. By the analysis of Ref. [28] we conclude that the function $X(v,w)$ has the expansion

$$X(v,w) = X(0,w) + \tfrac{2}{3}v + o(v), \tag{4.10}$$

and the function $Z(v,w)$ has the expansion

$$Z(v,w) = Z(0,w) + \tfrac{2}{3}v + o(v). \tag{4.11}$$

The term linear in v in both expressions is independent of w, and is identical to that found in the limit $w \to 0$. On the other hand, we find from Eq. (3.16) in the perfect-slip limit $w \to \infty$

$$X_s = \tfrac{1}{4} - \tfrac{2}{3}v + O(v^2), \quad Z_s = -\tfrac{1}{2} + \tfrac{2}{3}v + O(v^2). \tag{4.12}$$

This shows that for motion parallel to the wall the behavior is singular in the perfect-slip limit.

V. SPECTRUM OF BROWNIAN MOTION

In the theory of Brownian motion the velocity-correlation functions of a Brownian particle are defined by

$$C_{\alpha\beta}(t) = \langle U_\alpha(t) U_\beta(0) \rangle, \tag{5.1}$$

where the angular brackets denote the equilibrium ensemble average. We define the one-sided Fourier transform as

$$\hat{C}_{\alpha\beta}(\omega) = \int_0^\infty e^{i\omega t} C_{\alpha\beta}(t)dt. \tag{5.2}$$

According to the fluctuation-dissipation theorem [37] the Fourier transform is given by

$$\hat{C}_{\alpha\beta}(\omega) = k_B T \mathcal{Y}_{\alpha\beta}(\omega), \tag{5.3}$$

where k_B is Boltzmann's constant and T is the absolute temperature. In experiment one measures the position fluctuations of a Brownian particle confined to a trap. For definiteness we consider only the component of motion parallel to the x axis. The spectral density of thermal position fluctuations is given by

$$\langle x_\omega x^*_{\omega'} \rangle = \frac{k_B T}{\pi\omega}[\mathrm{Im}\chi_{xx}(\omega)]\delta(\omega - \omega'), \tag{5.4}$$

where the susceptibility tensor $\boldsymbol{\chi}(\omega)$ is related to the admittance tensor by

$$\boldsymbol{\mathcal{Y}}(\omega) = -i\omega\boldsymbol{\chi}(\omega). \tag{5.5}$$

The spectral density of position fluctuations is given by

$$S(\omega) = \frac{2k_B T}{\omega}\mathrm{Im}\chi_{xx}(\omega). \tag{5.6}$$

This can be evaluated from Eq. (2.8). In the limit of zero frequency one finds the value

$$S(0) = 2k_B T\frac{\zeta_{xx}(0)}{k^2}, \tag{5.7}$$

with steady-state friction coefficient

$$\zeta_{xx}(0) = \zeta_0\left[1 + \frac{3a}{2h}X(0,w)\right]^{-1}, \tag{5.8}$$

where $\zeta_0 = 6\pi\eta a$ is the Stokes friction coefficient for the bulk fluid. One sees from Eqs. (4.6) and (4.7) that the wall enhances the spectral density at zero frequency with respect to the bulk for the no-slip condition, and reduces the spectral density for the perfect-slip condition. It follows from Eq. (4.10) that in both cases the spectral density increases with frequency at low frequency. It tends to a peak near $\omega_0 = \sqrt{k/(m_p + \frac{1}{2}m_f)}$, before decreasing to zero.

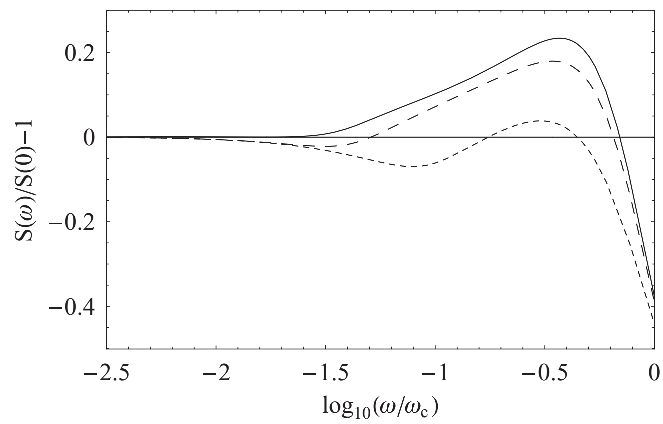

FIG. 2. Reduced spectral density $S(\omega)/S(0) - 1$ as a function of $\log_{10}(\omega/\omega_c)$ for a Brownian particle of radius a at distances $h = 5a$ (solid curve), $h = 7a$ (long dashes), and $h = 9a$ (short dashes) from a planar wall with partial-slip boundary condition. The parameter values are listed in Sec. V.

In the recent experiment of Jannasch *et al.* [16], it was found that the spectral density at first decreases with frequency, in contrast to the behavior found above. We have suggested [19] that this can be explained by assuming a frequency-dependent slip length $b(\omega)$ that vanishes at zero frequency and tends to a constant at higher frequency. Somewhat more generally we assume a dynamic slip length of the form

$$b(\omega) = b_0 + \frac{i\omega\tau_s}{1 - i\omega\tau_s}(b_0 - b_\infty), \tag{5.9}$$

characterized by three parameters b_0, b_∞, and τ_s.

In Fig. 2 we plot the reduced spectral density $S(\omega)/S(0) - 1$ for a Brownian particle of radius $a = 0.51$ μm and density $\rho_p = 2500$ kg m^{-3}, at reduced distances $h/a = 5,7,9$, in a fluid with density $\rho = 1000$ kg m^{-3} and shear viscosities $\eta = 0.705, 0.691, 0.637$ cP, as communicated by the authors of [16], with values of the spring constant characterized by $\omega_c = k/\zeta_0 = 2\pi f_c$ with $f_c = 71.54, 148.2, 156.9$ kHz, and slip length characterized by $b_0 = 10$ nm, $b_\infty = 1$ mm, and $\tau_s = 10^{-7}$ s. In Fig. 3 we plot $\log_{10}|S(\omega)/S(0) - 1|$ for the same values. This shows clearly the zeros of $S(\omega) - S(0)$. There is a similarity with similar plots of Jannasch *et al.* [16], but for the chosen values the spectral density for the nearest distance $h = 5a$ shows a minimum and a maximum, whereas for the experimental data for this case there is no extremum. It is necessary to choose $b_0 \ll b_\infty$ to cause a decrease of $S(\omega)$ at low frequency and produce the first zero crossing of $S(\omega) - S(0)$. The spectral density shows a strong dependence on the parameters in Eq. (5.9). In Fig. 4 we compare with the reduced spectral density $S(\omega)/S(0) - 1$ for $b_0 = 10$ nm, $b_\infty = 10$ μm, and $\tau_s = 10^{-7}$ s, and in Fig. 5 for $b_0 = 10$ nm, $b_\infty = 1$ mm, and $\tau_s = 10^{-4}$ s, but otherwise the same values. The plots in Fig. 2 suggest that a large slip length b_∞ is required if the data [16] are to be explained in the framework of the present theory. It may be preferable to regard the inverse of

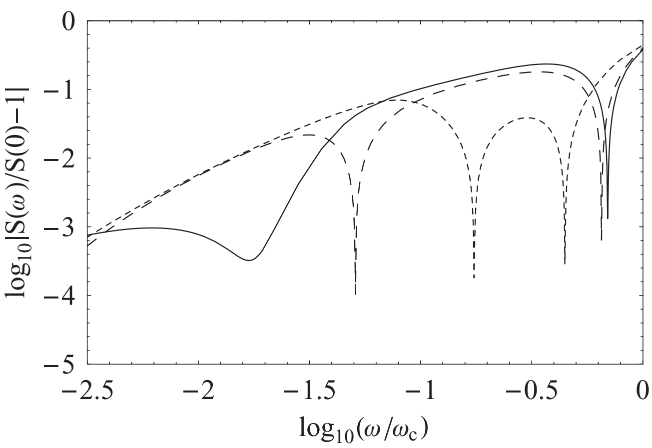

FIG. 3. $\log_{10}|S(\omega)/S(0)-1|$ as a function of $\log_{10}(\omega/\omega_c)$ for the same values as in Fig. 2.

the slip length as the physical quantity of interest [38]. A large b_∞ corresponds to near frictionless sliding at high frequency.

The slip length may be defined from the ratio $f=\sigma/v_s$, where σ is the shear stress at the wall and v_s is the fluid velocity at the wall [39]. The slip length is defined as $b=\eta/f$. In most cases with simple fluids the slip length is of the order of the molecular diameter, but for polymer melts and for a hydrophobic wall the slip length can become large. de Gennes [39] has suggested that in the latter case a gaseous film may form at the liquid/solid interface, and has estimated the slip length from a kinetic theory calculation. A dynamic mechanism involving nanobubbles at the wall, and leading to a frequency-dependent slip length, has been proposed by Lauga and Brenner [40]. In their model the friction f vanishes altogether at high frequency. They estimate a relaxation time of order 1 ms or less in connection with an experiment by Zhu and Granick [30]. It has been suggested by Granick [3] that collective two-dimensional motions near the wall can be responsible for a long relaxation time. It must be expected that surface stiffness and surface mass affect the frequency dependence [41].

It is useful to consider the total fluid momentum in the point-particle limit [42] in order to check that a dynamic slip length of the form Eq. (5.9) is physically possible. The total

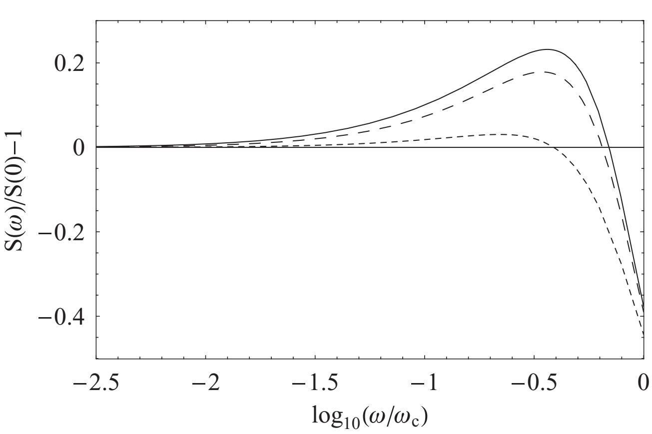

FIG. 4. As in Fig. 2, but for a smaller value of the slip length b_∞, as detailed in Sec. V.

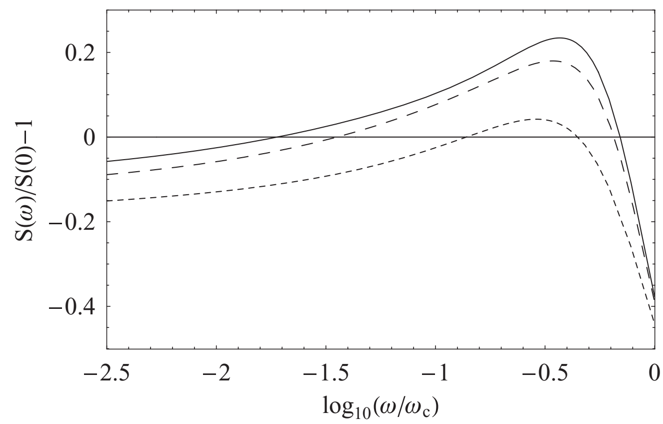

FIG. 5. As in Fig. 2, but for a larger value of the slip relaxation time τ_s, as detailed in Sec. V.

fluid momentum generated by the time-dependent force $\boldsymbol{E}(t)$ acting on a point particle located at $\boldsymbol{r}_0$ has the Fourier transform

$$\boldsymbol{P}_\omega(\boldsymbol{r}_0)=\boldsymbol{\Gamma}(\boldsymbol{r}_0,\omega)\cdot\boldsymbol{E}_\omega. \tag{5.10}$$

with the tensor [43]

$$\boldsymbol{\Gamma}(\boldsymbol{r}_0,\omega)=\rho\int_{z>0}\mathsf{G}(\boldsymbol{r},\boldsymbol{r}_0,\omega)\,d\boldsymbol{r}. \tag{5.11}$$

In the spatial Fourier representation Eq. (3.4), the integration over the horizontal coordinates x and y leads to a delta function $\delta(\boldsymbol{q})$ in the wave vector $\boldsymbol{q}=(q_x,q_y)$. It can be checked from the explicit expression for the transformed Green function $\hat{\mathsf{G}}(\boldsymbol{q},z,z_0,\omega)$ at $\boldsymbol{q}=\boldsymbol{0}$ that the tensor $\boldsymbol{\Gamma}(\boldsymbol{r}_0,\omega)$ is diagonal with equal elements $\Gamma_{xx}=\Gamma_{yy}$ and $\Gamma_{zz}=0$. In fact, a similar statement is valid before the integration over z. The element Γ_{xx} is given by

$$\Gamma_{xx}(\boldsymbol{r}_0,\omega)=\frac{1}{-i\omega}\left[1-\frac{e^{-\alpha h}}{1+\alpha b}\right]. \tag{5.12}$$

Substituting here $b=b(\omega)$, as given by Eq. (5.9), we obtain

$$\Gamma_{xx}(\boldsymbol{r}_0,\omega)=\frac{1}{-i\omega}\left[1-\frac{1+\alpha^2\nu\tau_s}{1+\alpha b_0+\alpha^2\nu\tau_s(1+\alpha b_\infty)}\,e^{-\alpha h}\right], \tag{5.13}$$

where $\nu=\eta/\rho$ is the kinematic viscosity. For positive values of the parameters the cubic in α in the denominator has positive coefficients. This implies that one zero of the cubic is negative and the other two zeros are each other's complex conjugates. Moreover, one of the complex zeros lies in the sector $\pi/3<\varphi<2\pi/3$ of the complex α plane. This behavior guarantees that after an initial impulse $\boldsymbol{E}(t)=\boldsymbol{P}_0\delta(t)$ the fluid momentum $\boldsymbol{P}(t)$ decays as a function of time [44]. More generally, b_0 can be negative [45], but the argument of the first complex zero of the cubic must be in the sector $\pi/4<\varphi<\pi$.

VI. COMPRESSIBLE FLUID

The theory can be extended to compressible fluids. This is relevant for dense gases and computer simulation fluids. The modification of the admittance $\mathcal{Y}_0(\omega)$ due to fluid compressibility has been described elsewhere [20,46]. The expressions for the reaction field factors F_{xx} and F_{zz} for a wall with no-slip boundary condition and a compressible fluid have been derived earlier [20]. For a wall with perfect-slip boundary condition the reaction field factors are easily derived by the method of images from the Green function G_0 for an infinite compressible fluid [47]. Here we present the reaction field factors for a compressible fluid and a wall with partial-slip boundary condition. The effect of a partial-slip boundary condition in viscous compressible hydrodynamics in other geometries has been studied by Erbas *et al.* [48].

We introduce the notation

$$\beta = \frac{\omega}{\rho_0 c_0^2}, \quad \mu = \frac{\omega}{c}, \quad c = c_0\left[1 - i\beta\left(\frac{4}{3}\eta + \eta_v\right)\right]^{1/2}, \tag{6.1}$$

where ρ_0 is the mean fluid density, c_0 is the long-wave sound velocity, c is the frequency-dependent sound velocity, and η_v is the volume viscosity. Instead of Eq. (3.8) we use the abbreviations [28]

$$n = \exp[rh], \quad u = \exp[sh], \quad s = \sqrt{q^2 + \alpha^2}, \tag{6.2}$$

where in the definition of α in Eq. (2.3) we must replace ρ by ρ_0, and r is defined by

$$r = \sqrt{q^2 - \mu^2}. \tag{6.3}$$

The reaction field factors take the form of Eqs. (3.5)–(3.7). The numerator $N_x(q,\omega)$ takes the form

$$\begin{aligned} N_x(q,\omega) = {} & 4nuq^2rs^2(1+sb) - u^2q^2s[q^2(1-rb) \\ & + rs(1+sb)](1+sb) + n^2r\{q^2s[r(1-3s^2b^2) \\ & - 2s^2b] - q^4(1+rb)(1-sb) - 2rs^3(1-s^2b^2)\}. \end{aligned} \tag{6.4}$$

The denominator $D_x(q,\omega)$ takes the form

$$\begin{aligned} D_x(q,\omega) = {} & 2n^2u^2rs(q^2-s^2)(1+sb) \\ & \times [q^2(1+rb) - rs(1+sb)]. \end{aligned} \tag{6.5}$$

The numerator $N_z(q,\omega)$ takes the form

$$\begin{aligned} N_z(q,\omega) = {} & 4nuq^2rs - u^2rs[q^2(1-rb) + rs(1+sb)] \\ & - n^2q^2[q^2(1+rb) + rs(1-sb)]. \end{aligned} \tag{6.6}$$

The denominator $D_z(q,\omega)$ takes the form

$$D_z(q,\omega) = n^2u^2s(q^2-s^2)[q^2(1+rb) - rs(1+sb)]. \tag{6.7}$$

For $b = 0$ these expressions reduce to those given in Ref. [28], apart from a common factor of -1. In the limit of an incompressible fluid they reduce to those given in Sec. III apart from a common factor of q. In the steady-state limit and at low frequency one obtains exactly the same expressions as in Sec. IV.

The tensor element $H_{xx}(\boldsymbol{r},\boldsymbol{r}_0,\omega)$ takes again the value Eq. (5.13), independent of the compressibility. The tensor element $\Gamma_{zz}(\boldsymbol{r},\boldsymbol{r}_0,\omega)$ becomes

$$\Gamma_{zz}(\boldsymbol{r},\boldsymbol{r}_0,\omega) = \frac{1}{-i\omega}[1 - e^{ih\mu}], \tag{6.8}$$

independent of the slip length.

We have checked that for a wall with partial-slip boundary condition the Green function satisfies the reciprocity relation

$$\mathsf{G}(\boldsymbol{r},\boldsymbol{r}_0,\omega) = \widetilde{\mathsf{G}}(\boldsymbol{r}_0,\boldsymbol{r},\omega), \tag{6.9}$$

where the tilde indicates transposition of the tensor. The relation was derived earlier for general confined geometry with the no-slip boundary condition [47]. It was used to simplify calculations of fluid dynamics in situations with one or two planar walls [43].

VII. DISCUSSION

The analysis shows that the concept of a frequency-dependent slip length may be useful for the description of dynamic surface phenomena in liquids. Whether it provides the correct explanation of the recent experiment [16] on the spectral density of Brownian motion remains to be seen. Further experimental work and computer simulations are desirable. The theoretical framework developed above provides a clear prediction in a wide range of circumstances.

A striking result of the recent experiment [16] is the initial decrease with frequency of the spectral density of Brownian motion. In the present theory this requires that the high-frequency value b_∞ of the dynamic slip length is larger than the low-frequency value b_0. This feature has been confirmed in computer simulations [41]. The result is also suggested by the measured strong increase of the slip length with shear rate [29,30] combined with an argument due to Zwanzig [31].

The main point of the above analysis is the calculation of the effect of a wall with partial-slip boundary condition on the motion of a particle at a distance from the wall large compared to its radius. The fluid can be incompressible or compressible. The observed motion can serve as a tool of investigation of the boundary condition. The motion can be extracted from the analysis of Brownian motion of a particle confined to a harmonic optical trap, or it can be observed more directly in atomic force microscopy with a tip at large distance from the wall. The theoretical analysis allows in particular the study of the frequency dependence of the boundary condition [40].

[1] G. K. Batchelor, *An Introduction to Fluid Dynamics* (Cambridge University Press, Cambridge, 1967).
[2] E. Lauga, M. P. Brenner, and H. A. Stone, in *Handbook of Experimental Fluid Dynamics*, edited by J. Foss, C. Tropea, and A. Yarin (Springer, New York, 2005), Chap. 15.
[3] S. Granick, Science **253**, 1374 (1991).
[4] S. Granick, Phys. Today **52**(7), 26 (1999).
[5] R. Pit, H. Hervet, and L. Léger, Phys. Rev. Lett. **85**, 980 (2000).
[6] L. Bocquet and J.-L. Barrat, Phys. Rev. Lett. **70**, 2726 (1993).
[7] L. Bocquet and J.-L. Barrat, Phys. Rev. E **49**, 3079 (1994).
[8] J.-L. Barrat and L. Bocquet, Phys. Rev. Lett. **82**, 4671 (1999).
[9] C. Neto, D. Evans, E. Bonnacurso, H.-J. Butt, and V. J. Craig, Rep. Prog. Phys. **68**, 2859 (2005).

[10] L. Bocquet and J.-L. Barrat, Soft. Matter **3**, 685 (2007).
[11] J. C. T. Eijkel and A. van den Berg, Microfluid. Nanofluid. **1**, 249 (2005).
[12] L. Bocquet and E. Charlaix, Chem. Soc. Rev. **39**, 1073 (2010).
[13] S. Jeney, B. Lukić, J. A. Kraus, T. Franosch, and L. Forró, Phys. Rev. Lett. **100**, 24004 (2008).
[14] T. Franosch and S. Jeney, Phys. Rev. E **79**, 031402 (2009).
[15] T. Franosch, M. Grimm, M. Belushkin, F. M. Mor, G. Foffi, L. Forró, and S. Jeney, Nature (London) **478**, 85 (2011).
[16] A. Jannasch, M. Mahamdeh, and E. Schäffer, Phys. Rev. Lett. **107**, 228301 (2011).
[17] S. F. Tolić-Nørrelyke, E. Schäffer, J. Howard, F. Pavone, F. Jülicher, and H. Flyvbjerg, Rev. Sci. Instrum. **77**, 103101 (2006).
[18] B. U. Felderhof, J. Phys. Chem. B **109**, 21406 (2005). We remark that the factor 3 in the high-frequency behavior given by Eq. (4.4) should be replaced by 1. See also the Erratum [B. U. Felderhof, J. Phys. Chem. B **110**, 13304(E) (2006)].
[19] B. U. Felderhof (to appear in J. Chem. Phys.).
[20] B. U. Felderhof, J. Chem. Phys. **123**, 184903 (2005).
[21] E. Lauga and T. M. Squires, Phys. Fluids **17**, 103102 (2005).
[22] A. Saugey, L. Joly, C. Ybert, J. L. Barrat, and L. Bocquet, J. Phys.: Condens. Matter **17**, S4075 (2005).
[23] H. A. Lorentz, Zittingsversl. Akad. Wet. **5**, 168 (1896); *Abhandlungen über Theoretische Physik* (Teubner, Leipzig, 1907), Vol. I, p. 40.
[24] S. Kim and S. J. Karrila, *Microhydrodynamics: Principles and Selected Applications* (Butterworth-Heinemann, Boston, 1991), Chap. 6.
[25] A. Sommerfeld, Ann. Phys. (Leipzig) **28**, 665 (1909).
[26] A. Sommerfeld, *Partielle Differentialgleichungen der Physik* (Deutsch, Thun, 1978), Chap. 6.
[27] R. B. Jones, J. Chem. Phys. **121**, 483 (2004).
[28] B. U. Felderhof, J. Chem. Phys. **124**, 054111 (2006).
[29] P. A. Thompson and S. M. Troian, Nature (London) **389**, 360 (1997).
[30] Y. Zhu and S. Granick, Phys. Rev. Lett. **87**, 096105 (2001).
[31] R. Zwanzig, Physica A **118**, 427 (1983).
[32] G. Sun, E. Bonaccurso, V. Franz, and H.-J. Butt, J. Chem. Phys. **117**, 10311 (2002).
[33] A. Maali and B. Bushan, Phys. Rev. E **78**, 027302 (2008).
[34] B. U. Felderhof and R. B. Jones, Physica A **136**, 77 (1986).
[35] B. U. Felderhof, Physica A **166**, 492 (1990).
[36] D. Frydel and S. A. Rice, Mol. Phys. **104**, 1283 (2006).
[37] E. H. Hauge and A. Martin-Löf, J. Stat. Phys. **7**, 259 (1973).
[38] A. Niavarani and N. V. Priezjev, Phys. Rev. E **77**, 041606 (2008).
[39] P. G. de Gennes, Langmuir **18**, 3413 (2002).
[40] E. Lauga and M. P. Brenner, Phys. Rev. E **70**, 026311 (2004).
[41] N. Asproulis and D. Drikakis, Phys. Rev. E **84**, 031504 (2011). The coefficient f in their Eq. (7) should have the opposite sign (private communication).
[42] B. Cichocki and B. U. Felderhof, Phys. Rev. E **62**, 5383 (2000).
[43] B. U. Felderhof, J. Chem. Phys. **133**, 074707 (2010).
[44] H. S. Carslaw and J. C. Jaeger, *Conduction of Heat in Solids* (Clarendon Press, Oxford, 1959), p. 494.
[45] N. V. Priezjev, J. Chem. Phys. **127**, 144708 (2007).
[46] D. Bedeaux and P. Mazur, Physica A **78**, 505 (1974).
[47] R. B. Jones, Physica A **105**, 395 (1981).
[48] A. Erbas, R. Podgornik, and R. R. Netz, Eur. Phys. J. E **32**, 147 (2010).